The cue-reactivity paradigm: An ensemble of networks driving attention and cognition when viewing drug-related and natural-reward stimuli

Lauren D. Hill-Bowen[1], Michael C. Riedel[2], Ranjita Poudel[1], Taylor Salo[1], Jessica S. Flannery[1], Julia A. Camilleri[3,4], Simon B. Eickhoff[3,4], Angela R. Laird[2], and Matthew T. Sutherland[1]*

[1] Department of Psychology, Florida International University, 11200 SW 9th Street, Miami, FL, 33199, United States
[2] Department of Physics, Florida International University, 11200 SW 9th Street, Miami, FL, 33199, United States
[3] Institute of Neuroscience and Medicine, Brain & Behaviour (INM-7), Research Centre Jülich, 52425 Jülich, Germany
[4] Institute of Systems Neuroscience, Medical Faculty, Heinrich Heine University Düsseldorf, 40225 Düsseldorf, Germany

***Correspondence:**
Matthew T. Sutherland, Ph.D.
Florida International University
Department of Psychology
AHC-4, RM 312
11299 SW 8th St
Miami, FL 33199
masuther@fiu.edu
305-348-7962

KEYWORDS: cue-reactivity, functional connectivity, hierarchical clustering, meta-analytical connectivity modeling

ABSTRACT

Background: The cue-reactivity paradigm is a widely adopted neuroimaging probe assessing brain activity linked to attention, memory, emotion, and reward processing associated with the presentation of appetitive stimuli. Lacking, is the apperception of more precise brain regions, neurocircuits, and mental operations comprising cue-reactivity's multi-elemental nature. To resolve such complexities, we employed emergent meta-analytic techniques to enhance insight into drug and natural cue-reactivity in the brain.

Methods: Operating from this perspective, we first conducted multiple coordinate-based meta-analyses to define common and distinct brain regions showing convergent activation across studies involving drug-related and natural-reward cue-reactivity paradigms. In addition, we examined the activation profiles of each convergent brain region linked to cue-reactivity as seeds in task-dependent and task-independent functional connectivity analyses. Using methods to cluster regions of interest, we categorized cue-reactivity into cliques, or sub-networks, based on the functional similarities between regions. Cliques were further classified with psychological constructs.

Results: We identified a total of 164 peer-reviewed articles: 108 drug-related, and 56 natural-reward. When considering cue-reactivity collectively, across both drug and natural studies, activity convergence was observed in the dorsal striatum, limbic, insula, parietal, occipital, and temporal regions. Common convergent neural activity between drug and natural cue-reactivity was observed in the caudate, amygdala, thalamus, cingulate, and temporal regions. Drug distinct convergence was observed in the putamen, cingulate, and temporal regions, while natural distinct convergence was observed in the caudate, parietal, occipital, and frontal regions. We seeded identified cue-reactivity regions in meta-analytic connectivity modeling and resting-state functional connectivity analyses. Consensus hierarchical clustering of both connectivity analyses identified six distinct cliques that were further functionally characterized using the BrainMap and Neurosynth databases.

Conclusions: We examined the multifaceted nature of cue-reactivity and decomposed this construct into six elements of visual, executive function, sensorimotor, salience, emotion, and self-referential processing. Further, we demonstrated that these elements are supported by perceptual, sensorimotor, tripartite, and affective networks, which are essential to understanding the neural mechanisms involved in the development and or maintenance of addictive disorders.

INTRODUCTION

The cue-reactivity paradigm is commonly adopted in neuroimaging research to assess neurobiological processes linked with craving, reward, and behavioral motivation, particularly, in addiction, to probe the incentive salience of drugs, and their associated cues [1-3]. The basis of the cue-reactivity paradigm is that previously associated cues to the drug, or natural stimuli (i.e., food), can under certain conditions, evoke stimulus-associated responses such as urge to use drug or urge to eat [4]. In essence, the cue signals the drug, or natural stimuli, which in turn activates reward circuitry and triggers physiological arousal and anticipation. Cue-reactivity can be symbolic-expressive (e.g., craving) [5], physiological (e.g., sweating, salivation), and/or behavioral (e.g., drug-seeking, consumption) [6]. As cue-reactivity engages multiple systems involved in attention, memory, and reward, the specific neural mechanisms associated with each system has yet to be comprehensively defined across both drug-related and natural-rewards. Delineating these neural systems involved in cue-reactivity has important implications for understanding addiction, where the coupling of heightened cue-responses and increased attention to addiction-related cues is a key mechanism in the development and/or maintenance of addictive behaviors [7]. A recent review of factors predicting relapse and sustained abstinence in substance use disorder found greater activation to drug cues was predictive of worse clinical outcomes, yet greater activation to non-drug cues was linked with better outcomes [8]. Research continuously features cue-reactivity as a task essential in understanding substance addiction, relapse rates, and clinical outcomes, yet parsing out the multifaceted nature of cue-reactivity, including craving, reward, and motivation, remains to be more fully characterized within both drug and natural rewards.

Cue-responsivity elicits increased blood-oxygenation level-dependent (BOLD) signals in brain regions linked with subjective value, as well as attentional, and motivational processes that govern behavior [9]. This is supported by accumulating evidence demonstrating positive

correlations between regional cue-related activation and measures of self-reported craving [10]. As it relates to drug cue-reactivity, the presentation of drug-related cues has been shown to reliably engage neural circuits involved in learning and memory, as well as reward/motivation networks, including the mesocorticolimbic and nigrostriatal dopaminergic systems [11]. Activation of the mesocorticolimbic system correlates with drug-seeking and drug-taking behaviors that is characterized by an increase in extracellular dopamine concentration [12], while activation of the nigrostriatal system is essential for habit learning and automaticity of behavior [13]. Specifically, dopamine projections between the prefrontal cortex (PFC) and the dorsolateral striatum are critical in the development of habits, and when considering drug use, these projections enhance the conditioned reinforcement mechanisms promoting the habituation of drug-seeking and drug-taking behavior. Research supports that not only are these systems engaged during drug cue-reactivity, but also during natural-reward cue-reactivity, suggesting common mechanisms involved in assigning value to stimuli and transforming subjective valuations into behavioral action signals [14].

An entrenched view is that repeated drug use "hijacks" the brain's reward system that has evolved to maintain the survival of the organism and species by playing a critical role in reinforcing consummatory and procreative behaviors [12, 15, 16]. Addictive drugs produce a greater magnitude and longer-lasting concentration of synaptic dopamine than natural rewards, leading to a profound remodeling of these systems following extended use [17]. Extensive evidence supports the notion that drugs of abuse usurp natural reward mechanisms via neurotransmitter system modulations [18, 19], region-to-region functional interactions involved in reward learning [20], and neuronal morphology [21, 22] specifically in cortical, striatal, and brain stem regions. Initially, drug intake is an unconditioned stimulus, but with repeated use a drug cue becomes a conditioned stimulus that is predictive of a drug response [23]. With drug cues as a conditioned stimulus, they

elicit dopamine release associated with reward prediction [24], thus "hijacking" the natural reward system. Delineating these distinct, "hijacked" regions by drugs of abuse, as well as conversely regions preserved in natural reward systems has potential to inform neurobiological models of addiction.

The distinct neural processes involved in the commonly used cue-reactivity paradigm, given its multifaceted nature, have not yet been fully delineated from a neuroimaging perspective. Additionally, a comprehensive understanding of the common and distinct neurobiological attributes of drug-cue reactivity and natural reward processing is also lacking. Neuroimaging meta-analytic techniques offer a means to combine neuroimaging results across the literature to achieve consensus views. Previous cue-reactivity meta-analyses have focused on a range of substances (e.g., nicotine, alcohol, cocaine, heroin, and cannabis) and determined that the ventral striatum (VS), amygdala, PFC, visual cortex, and anterior cingulate cortex (ACC) are consistently more active during drug-related stimuli presentation than control stimuli presentation [9, 10, 25-29]. Natural reward meta-analyses focusing on the neural response to food, sex, and gambling cues among healthy drug-free adults have found the VS, ventromedial prefrontal cortex (vmPFC), amygdala, anterior insula, and mediodorsal thalamus [30, 31] as regions consistently more active during natural cue presentation than control cue presentation. Qualitatively, regions demonstrating increased activation in both reward systems include the VS, amygdala, and prefrontal cortex.

The current study seeks to expand on this prior meta-analytic work and provide enhanced insight into the brain regions and associated neurobiological networks underlying cue-reactivity and their more precise roles in drug and natural reward systems. The first aim was to identify common and distinct regions of convergent activity increases from drug-related and natural-reward studies. The second aim was to employ both resting-state functional connectivity (rsFC) and meta-analytic co-activation modeling (MACM) to examine task-independent, and task-dependent

functional connectivity for identified cue-related regions of interest. Finally, the third aim was to categorize cue-reactivity into cliques, or sub-networks, and define each clique with specific behavioral phenomena.

METHODS

Functional MRI search strategy and study selection. We conducted an extensive literature search to compile a comprehensive corpus of peer-reviewed visual cue-reactivity functional magnetic resonance imaging (fMRI) studies on drugs of abuse and natural rewards that were published up until 08/31/2017. In the first iteration, we searched multiple databases, including *Google Scholar* (https://scholar.google.com) and *PubMed* (https://www.ncbi.nlm.nih.gov/pubmed) for peer-reviewed articles indexed by the combination of keywords: ("cue-reactivity" OR "drug cue" OR "natural cue") AND ("fMRI" OR "GingerALE" OR "meta-analysis") AND/OR ("nicotine" OR "smoking" OR "cocaine" OR "cannabis" OR "heroin" OR "alcohol" OR "sexual" OR "sex" OR "food"). In the second iteration, candidate studies were identified through the bibliographies of recently published meta-analyses for subsequent articles not compiled from the database searches [3, 14, 30, 31]. In the final iteration, we examined the reference lists of relevant articles for additional studies not located by database searches or published meta-analyses.

The inclusion/exclusion criteria for the meta-analyses in the current study were as follows: a) articles that utilized fMRI task paradigms to asses drug and/or natural cue-reactivity with visual stimuli, other sensory paradigms such as gustation were excluded b) studies with reported activity foci as 3D coordinates (X, Y, Z) in stereotaxic Talairach or Montreal Neurological Institute (MNI) space, regions-of-interest (ROIs) derived from a parcellation scheme were excluded given the absence of coordinates c) experiments that performed whole brain (WB) or ROI analyses for the

within-subject contrast of drug cue > neutral or control cue stimuli, or natural cue > neutral or control cue stimuli, and finally, d) articles that reported subject-relevant demographic information such as age and male/female ratio, and data analytic methods including imaging modality and processing software (e.g., AFNI, FSL, SPM). All reported coordinates of activity foci that aligned with our inclusion and exclusion criteria were extracted for each experiment, as well as the corresponding behavioral data regarding participant age, male/female ratio, cue type (e.g., alcohol, cannabis, cocaine, heroin, nicotine, food, & sex), imaging modality, fMRI processing software, number of reported activation foci, contrast of interest for the original study, and analytic procedure (WB or ROI).

Regional activation of drug and natural cue-reactivity: meta-analytic procedures. We employed the revised version of the Activation Likelihood Estimation (ALE) algorithm (version 3.1) implemented in MATLAB version 8.2.0.701 (R2013b), a coordinate-based meta-analytic technique, to identify regions of convergent activation across and between drug-related and natural-reward cue-reactivity experiments. Activation foci reported in Talairach space in the original study were linearly transformed to MNI space [32]. The ALE algorithm is a voxel-wise approach that models brain activity foci as 3D Gaussian probability distributions centered at the given coordinate, where the width of the distribution represents sample size variance and uncertainty, to identify statistically significant spatial convergence [33-35]. The algorithm generated a set of modeled activation (MA) maps for each experimental contrast, where each voxel's value corresponded to the maximum probability from foci-specific maps, and then the voxel-wise union across all experimental contrasts was calculated, quantifying the spatial convergence across the brain. Significance testing was then applied to the resulting voxel-wise ALE value distributions by analytically deriving the null distribution of random spatial association between experiments [34]. For all analyses, a multiple comparisons correction was applied with a

cluster-forming threshold of $p_{voxel\text{-}level} < 0.001$ and a cluster-extent threshold of $p_{cluster\text{-}level} < 0.05$. Maps were exported to MANGO (http://ric.uthscsa.edu/mango/) for visualization on an anatomical (MNI152_T1_1mm_brain) template.

Coordinates from experiments having reported increases in activation for drug cues or natural cues, relative to neutral cue stimuli (i.e., drug > neutral, natural > neutral) were utilized in the following ALE meta-analyses. First, to assess *pooled* cue-reactivity convergence across stimuli types, coordinates from drug cue-reactivity and natural cue-reactivity experiments were collapsed to identify regions where reward cues were greater than neutral cues (i.e., drug and natural collapsed > neutral). Next, two separate ALE maps, one each for drug and natural cue-reactivity contrasts were calculated. The first map included drug cue-reactivity experiments where drug cues demonstrated increased activity relative to neutral cues (i.e., drugs > neutral), and the second map included natural cue-reactivity experiments where natural cues demonstrated increased activity relative to neutral cues (i.e., natural > neutral). Next, to ascertain regions that are *common* in both cue-reactivity paradigms, we performed a conjunction analysis of the two separate ALE maps using the minimum statistic approach [36]. The conjunction analysis results defined the overlap shared by both cue-reactivity paradigms (i.e., drugs AND natural cues). A final contrast was conducted to elucidate *distinct* convergence differences across stimuli categories and distinguish regions where drug cues showed greater convergent activation than natural cues, and vice versa (i.e., drugs > natural cues and natural > drug cues).

Following ALE meta-analyses, we extracted ROIs from the *pooled* cue-reactivity contrast results to subsequently identify "cliques", or sub-networks of functionally similar brain regions through ancillary analyses involving rsFC and MACM. Given that some clusters spanned across multiple brain regions, which may represent distinct functional nodes, we defined ROIs for subsequent analyses by generating 5-mm radius spherical seeds positioned at the local maxima

within each cluster. For this, we utilized FSL's *cluster* command and required that local maxima be distanced no less than 15-mm from each other. Three foci of local maxima were discarded because they were located at transitional anatomical locations (i.e., edge of the brain, cerebellar/occipital lobe boundary), making interpretation problematic during ancillary connectivity analyses.

Resting-state functional connectivity. For each ROI, seed-based rsFC was conducted to identify task-independent functional connectivity between the average ROI time-course, and the rest of the voxels in the brain. Resting-state fMRI data from the Nathan Kline Institute- Rockland Sample [37] was acquired for 192 healthy volunteers and re-analyzed by Heinrich-Heine University in Dusseldorf [38]. Participants were instructed to look at a fixation cross in the center of the screen and avoid falling asleep during acquisition. Data was collected with a Siemens 3T TrimTrio scanner using BOLD contrast (gradient-echo EPI pulse sequence; repetition time [TR] = 1.4 s; echo time [TE] = 3 ms; flip angle [FA] = 65º; voxel size = 2.0 mm x 2.0 mm x 2.0 mm, 64 slices).

To remove any artifacts due to physiology and/or movement, FIX was used (FMRIB's ICA-based Xnoiseifier, version 1.061 as implemented in FSL 5.0.9; [39, 40]) to auto-classify independent components analysis (ICA) components as either "signal" (i.e., brain activity) or "noise" (e.g., effects of motion, non-neuronal physiology) using a large number of distinct spatial and temporal features via pattern classification. Together with 24 motion parameters (i.e., derivatives and second order effects [41]), unique variance related to the "noise" independent components (ICs) were regressed from the data. Further preprocessing on the data was done using SPM8 (Wellcome Trust Centre for Neuroimaging, London) and Heinrich-Heine University in Dusseldorf in-house MATLAB (MathWorks Inc, Natick, Massachusetts) scripts. The first four scans were removed, and remaining EPI images were corrected for head motion using a two-pass

affine registration (alignment to initial volume, and alignment to the mean after first pass). For each subject, the mean EPI image was spatially normalized to ICBM-152 reference space using the unified segmentation approach [42], and then applied to individual EPI volumes. Images were then spatially smoothed with a 5-mm FWHM Gaussian kernel to compensate for residual anatomical variance and improve signal-to-noise ratio. Each seed time-course was extracted per subject by computing the first eigenvariate of the time-series of all voxels within 5-mm of the seed coordinate. The variance due to mean white matter and cerebral spinal fluid signal was removed from the time-course to reduce spurious correlations, and subsequently underwent band-pass filtering (.01-.08 Hz). Using Pearson (linear) correlation, the processed time-course for each seed was correlated with the time-series of all other gray-matter voxels in the brain, and resulting coefficients were Fisher Z-transformed (Z-images) for second-level group analyses (ANOVA) with age and gender as covariates of no interest. Non-parametric permutation-based inference and a threshold of $p < 0.05$ corrected for multiple comparisons at the cluster level was applied to the resulting data.

Meta-analytic co-activation modeling. Additionally, for each ROI we conducted MACM analyses. MACM examines the task-based functional connectivity of an ROI (i.e., seed region) by identifying co-activation patterns across neuroimaging literature and probing the associated behavioral domains of the analyzed tasks [43]. Co-activation patterns are defined as an above-chance convergence of experimentally reported foci in the neuroimaging literature reporting simultaneous activation along with a given seed region using statistical inference, thus defining functional connections [44]. MACM maps reflect the locations in the brain that are most likely to be co-activated with a given seed region across multiple task-states and behavioral domains. To do so, we utilized BrainMap [45, 46], a large-scale database comprised of previously published functional and structural neuroimaging experiments, and associated 3D stereotaxic coordinates

across both healthy and diseased individuals. Statistical significance was assessed at $p < 0.05$ after multiple comparisons correction [47].

Clustering of cue-reactivity regions. We performed hierarchical clustering on the rsFC profiles, as well as separately on the whole-brain co-activation (MACM) profiles for each ROI to identify cliques, or sub-networks involved in cue-reactivity. Hierarchical clustering groups similar elements (i.e., seed regions) into clusters in a stepwise manner, where seed regions within a cluster have the most similar features, yet individual clusters are maximally distinct. The algorithm does so by finding two clusters that are closest together, and merging the two most similar clusters until all clusters are merged together as measured by standardized Euclidean distances and Ward's incremental sum of squares method [48, 49]. Clustering results are illustrated by a dendrogram, and demonstrate distinct cliques within both rsFC, and MACM separately.

The FSLNets toolbox (https://fsl.fmrib.ox.ac.uk/fsl/fslwiki/FSLNets) was used to calculate rsFC between all ROIs. To estimate pairwise functional connectivity we calculated partial temporal correlations of all seed regions' time series data [50]. One-sample t-tests were conducted for each pairwise connection using Fisher's Z-transformed functional connectivity values, representing the connectivity strength and consistency across the sample. WARD clustering was then applied to the resulting standardized connectivity matrix. Both rsFC and MACM maps were entered into the hierarchical clustering algorithm un-thresholded for significance in order to preserve the full functional and connectivity patterns of each ROI.

Utilizing the separate hierarchical clustering results from the rsFC and MACM analyses, we sought to identify a unifying framework of cliques participating in the cue-reactivity paradigm. To do this, we evaluated the consistency of each seed region's assignment with other seed regions within cliques across rsFC and MACM clustering solutions using the Dice Similarity Coefficient. Pair-wise comparisons were made across seed regions, whereby if two seeds were assigned to the

same cluster in the rsFC and MACM analyses, the pairing would be assigned a Dice Similarity Coefficient (DSC) of 1. If the pair of seed regions were assigned to the same cluster in only one of the analyses, the pairing would be assigned a DSC of 0.5, and 0 if the two seed regions were never assigned to the same cluster in either solution. This resulted in a symmetric matrix of similarity coefficients, where the upper triangle of this matrix was interpreted as distances in a third hierarchal clustering analysis.

Functional classification of cue-reactivity cliques. Finally, the identified cliques from the consensus clustering solution between rsFC and MACM were functionally characterized based on BrainMap metadata describing the cognitive, perceptual, or motor process isolated by cue-reactivity using forward- and reverse-inference [43, 46, 51]. Metadata describing the experimental design and data processing pipeline has been curated for over 3,600 publications and 15,000 experiments, which have reported over 120,000 brain activation coordinates among more than 110,000 research participants. BrainMap classifies experiments by the behavioral domain (BD) and paradigm class (PC). The BD is the category and subcategory classifying the mental operations likely isolated by the contrast of functional data, and the PC is the experimental task used. Forward inference describes the likelihood that a specific region(s) of interest will activate given the recruitment of mental operations [P(Activation | Operation)], while reverse inference describes the likelihood that mental operations (e.g. cognition, action, emotion) are being recruited given activation in a seed region(s) of interest [P(Operation | Activation)]. Combined, these two techniques provide important information about the brain-behavior relationship [52]. In the forward inference approach, we tested whether the conditional probability of activation, given a mental operation, was higher than the baseline probability of activating the specific region(s) of interest [P(Activation)]. Statistical significance was calculated using a binomial test [$p < 0.05$, correct for multiple comparisons using false discovery rate (FDR)]. Alternatively, in the reverse

inference approach we identified the most likely behavioral domains, given activation in a specific region(s) of interest using Bayes' rule. Bayes' rule derives P(Operation | Activation) from P(Activation | Operation) as well as P(Operation) and P(Activation). Statistical significance was calculated using a Chi-square test ($p < 0.05$, correct for multiple comparisons using FDR). To complement the BrainMap metadata approach to functional characterization of cue-reactivity cliques, we performed a similar analysis using the Neurosynth database [52]. The methods describing these analyses are located in the Supplementary Information.

RESULTS

Literature Search. Following the outlined inclusion criteria, a total of 164 peer-reviewed articles were identified: 108 drug cue-reactivity (3,994 subjects), and 56 natural cue-reactivity (1,730 subjects) (**Table S1 & S2**). A PRISMA flow diagram depicting the literature search and selection process of the included and excluded studies is provided in **Supplemental, Figure S1**. The 108 drug cue-reactivity studies can be further categorized based on specific substance of interest: 40 nicotine, 33 alcohol, 12 cocaine, 13 cannabis, and 10 heroin. Similarly, the 56 natural cue-reactivity studies can be further categorized based on specific cue stimuli of interest: 35 sexual and 21 food. The total number of foci/coordinates extracted from drug cue-reactivity studies was 1,418, while the total number extracted from natural cue-reactivity studies was 1,077. On average, subjects from articles included in the drug cue-reactivity analyses were 32.5 ± 9.0 (mean ± SD) years old and consisted of 2,757 males and 1,237 females, while subjects from articles included in the natural cue-reactivity analyses were 27.9 ± 7.1 (mean ± SD) years old and consisted of 793 males and 937 females.

Pooled, common, and distinct regions of convergence. First, we sought to enhance insight into the neural processing of drug *and* natural cue-reactivity. As such, we conducted a *pooled* meta-analysis identifying regions of convergent activation across *both* cue-reactivity domains (i.e., drug and natural collapsed > neutral). Convergent brain activity, resulting from the ALE meta-analysis including local maxima within each cluster, was observed in 23 regions including bilateral inferior occipital and temporal, bilateral parietal, left inferior frontal, bilateral middle occipital, bilateral insula, left supramarginal, left cingulate, bilateral thalamus, bilateral amygdala, and bilateral dorsal striatum (**Fig. 1A; Table 1A**).

Next, we aimed to identify convergent neural activity in drug cue-reactivity, and natural cue-reactivity separately, as well as the convergent regions the two domains share in *common*. As such, we first conducted two separate ALE meta-analyses for each cue-reactivity stimulus domain. The drug cue ALE meta-analysis (i.e., drug > neutral cue) identified significant activity convergence in nine clusters including the bilateral caudate, right inferior occipital, and left cingulate, amygdala, thalamus, and temporal regions (**Fig. 1B**, gold). The natural cue ALE meta-analysis (i.e., natural > neutral cue) identified significant activity convergence in ten clusters including the right amygdala, bilateral middle occipital, bilateral inferior parietal and frontal, and left anterior cingulate regions (**Fig. 1B**, blue). We next conducted a conjunction analysis to illustrate *common* regions of convergent activity overlap for drug and natural cue-reactivity (i.e., drug > neutral AND natural > neutral). Common convergence between both cue-reactivity stimulus domains was observed in eight clusters, including the bilateral caudate, left amygdala, bilateral thalamus, left inferior temporal, and bilateral anterior cingulate regions (**Fig. 1B**, pink; **Table 1B**).

Finally, to elucidate *distinct* regions of convergent activation, or rather domain specificity for drug cue-reactivity and natural cue-reactivity, we performed two contrast analyses. When

considering drug distinct convergence (i.e., drug > natural cues), we identified four significant clusters in the left cingulate, and right putamen and inferior temporal regions (**Fig. 1C; Table 1C**). When considering natural distinct convergence (i.e., natural > drug cues), we identified eleven significant clusters in the right caudate, bilateral middle occipital, bilateral parietal, bilateral inferior and middle frontal, and left anterior cingulate (**Fig. 1D; Table 1D**).

Identification of cue-reactivity cliques. To examine the task-independent, and task-dependent functional profiles of 23 ROIs from the *pooled* cue-reactivity meta-analytic results we performed rsFC and MACM analyses for each seed region independently (**Fig. S2 & S3**). The resulting seed-based functional connectivity maps were then entered into the hierarchical clustering algorithm, providing a clustering solution for each task state, separately. Clustering solutions for rsFC patterns (**Fig. S4**) and MACM maps (**Fig. S5**) revealed primarily consistent cliques, with a few differences, across both task states (**Fig. 2**). Cliques were largely consistent across both solutions, where Clique 1 demonstrated activation patterns originating in occipital regions and shifts to more parietal-frontal regions in Cliques 2 and 3, and finally to more medial-limbic regions in Cliques 4-6. Only slight individual region derivations between the two solutions were present in Cliques 1 through 4; however, larger shifts of regional groupings in Cliques 5 and 6 differentiate the two solutions. Specifically, cingulate regions dominated Clique 6 in the MACM solution, where in the rsFC solution cingulate regions clustered with the caudate and thalamus. Further, amygdala regions clustered only with the putamen in rsFC Clique 5, where in MACM Clique 5 amygdala regions clustered with occipital, insula, and caudate regions.

To provide a unifying framework of cliques participating in the cue-reactivity paradigm, across both rsFC and MACM, we used the Dice Similarity Coefficient to create a consensus clustering solution between both domains. Results revealed six cliques comprising the cue-reactivity network (**Fig. 3**). Clique 1 (green) included bilateral inferior occipital and temporal

regions. Clique 2 (yellow) included bilateral inferior parietal regions, and right inferior frontal and middle occipital regions. Clique 3 (orange) included left insula, supramarginal, middle occipital, and inferior parietal regions. Clique 4 (purple) included left anterior cingulate, right putamen, and bilateral insula and thalamus regions. Clique 5 (blue) included bilateral amygdala. Clique 6 (red) included bilateral caudate, and left anterior and posterior cingulate regions.

Functional profiles of cliques. Using the BrainMap database metadata, we characterized the functional profiles of the six cue-reactivity cliques from the consensus clustering solution (**Fig. 3**, **Table S3**). Behavioral decoding results utilizing a comparable database, Neurosynth, are located in the supplemental material (**Table S4**). Both BrainMap and Neurosynth decoding results were carefully reviewed for consensus to guide the functional interpretations of the resultant cue-reactivity cliques each described below:

Clique 1 was composed primarily of occipital-temporal regions (green). BrainMap metadata convergence indicated significance correspondence in the forward and reverse analyses within behavioral domains associated with perceiving and observing simple and complex visual cues. Neurosynth decoding included functional terms of “visual”, “object”, “visual word”, “motion”, and “selective”, and anatomical terms of “occipito temporal”, “occipito”, “lateral occipital”, “fusiform”, and “extrastriate”. Coherence across results indicates that this clique was associated with visual and attentional processes.

Clique 2 primarily included parietal-occipital regions (yellow) with similar topological properties as the canonical central executive network. BrainMap metadata convergence indicated significance correspondence in the forward and reverse analyses within behavioral domains associated with perception of higher-level visual features including color, motion, and spatial location, as well as working memory and reasoning cognitive processes. Neurosynth decoding included functional terms of “task”, “attentional”, “working memory”, “visually”, and “target”,

and anatomical terms of “parietal”, “intraparietal”, “posterior parietal”, “fronto parietal”, and “superior parietal”. Coherence across results indicates that this clique was associated with executive functions across a range of visual and working memory tasks.

Clique 3 was composed of the insula and secondary somatosensory regions (orange). BrainMap metadata convergence indicated significance correspondence in the forward and reverse analyses within behavioral domains associated with internal and external bodily perceptions. Neurosynth decoding included functional terms of “somatosensory”, “painful”, “tactile”, “motor”, and “touch”, and anatomical terms of “secondary somatosensory”, “somatosensory cortices”, “insula”, “operculum”, and “primary secondary”. Coherence across results indicates that this clique was associated with sensory and motor processes.

Clique 4 included regions displaying similar topological properties as the canonical salience network (purple). BrainMap metadata convergence indicated significance correspondence in the forward and reverse analyses within behavioral domains associated with reward processing and interoception. Neurosynth decoding included functional terms of “reward”, “monetary”, “incentive”, “response”, and “motivation”, and anatomical terms of “anterior insula”, “insula”, “anterior cingulate”, “striatum”, and “thalamus”. Coherence across results indicates that this clique was associated with salience attribution.

Clique 5 was distinctly composed of the amygdala (blue). BrainMap metadata convergence indicated significance correspondence in the forward and reverse analyses within behavioral domains associated with processing emotions of disgust, fear, happiness, humor, and sadness. Neurosynth decoding included functional terms of “emotional”, “neutral”, “fear”, “valence”, and “affective”, and anatomical terms of “amygdala”, “hippocampus”, “limbic”, “amygdala insula”, and “orbitofrontal cortex”. Coherence across results indicates that this clique was associated with emotion processing.

Clique 6 the final clique, included regions with similar topological properties as the canonical default mode network, and caudate (red). BrainMap metadata convergence indicated significance correspondence in the forward and reverse analyses within behavioral domains associated with reward processing, as well as attentional and social cognitive processes. Neurosynth decoding included functional terms of "reward", "self-referential", "monetary", "value", and "default mode", and anatomical terms of "medial prefrontal", "striatum", "cingulate", "posterior cingulate", and "ventral striatum". Coherence across results indicates that this clique was associated with the default mode, specifically self-referential processes.

DISCUSSION

To investigate the multifaceted mental operations involved in drug and natural cue-reactivity, the current study aimed to expand on prior meta-analytic work by providing enhanced insight in the more precise brain networks and associated behavioral phenomena engaged during cue-reactivity tasks. We first aimed to identify pooled, common, and distinct regions of convergent activity in both drug and natural cue-reactivity studies. When considering cue-reactivity collectively, pooled activity convergence was observed in regions of the dorsal striatum, limbic system, insula, parietal, occipital, and temporal regions. Second, we aimed to examine the functional profiles, both task-free and task-based, of regions showing convergent activity during cue-reactivity. Finally, we aimed to identify cliques, or sub-networks from the functional profiles of cue-reactivity regions and subsequently define each clique with specific behavioral phenomena. Based on functional and behavioral profiles, we concluded that cue-reactivity is comprised of six cliques: visual, executive function, sensorimotor, salience, emotion, and self-referential.

Convergent and distinct regions in cue-reactivity. When examining convergent brain regions involved in cue-reactivity across both drug and natural stimuli, *pooled* meta-analytic

outcomes identified the ACC, posterior cingulate cortex (PCC), caudate, amygdala, thalamus, insula, putamen, parietal, occipital, temporal, and somatosensory as regions of convergence across the cue-reactivity literature. Our findings largely replicate Noori and colleagues' (2016) results across both natural (food and sex) and drug (alcohol, cannabis, cocaine, heroin, and nicotine) cues compared to contrast cues in the striatum, ACC, PCC, inferior/superior parietal lobule, insula, middle occipital gyrus (MOG), and inferior temporal gyrus (ITG) [14]. The primary distinction between our current findings and Noori and colleagues' (2016) findings are that they report additional regions of convergent activation in the precentral gyrus (BA 6), cingulate gyrus (BA 24), medial frontal gyrus (BA 10), and claustrum. When examining *common* meta-analytic outcomes, we observed overlap between drug and natural cue-reactivity in the caudate, amygdala, thalamus, ITG, and regions of the ACC. Our results replicate Noori and colleagues' (2016) findings in the common network in the caudate, amygdala, and the ACC and extend results to the thalamus and ITG.

Additionally, we established regions where drugs of abuse produce greater convergence of activation compared to natural cues, thus defining regions where drugs of abuse potentially usurp these naturally rewarding systems. The meta-analytic outcomes for the contrast analysis specifying drug *distinct* convergence identified the PCC, putamen, fusiform gyrus, and ACC as regions recruited by drugs of abuse in the brain. These outcomes are consistent with a previous alcohol drug specific cue-reactivity meta-analysis reporting robust activation in the ACC, PCC, and temporal regions [28]; as well as a previous nicotine drug specific cue-reactivity meta-analysis reporting robust activation in the ACC, PCC, and dorsal striatum [25]. The PCC, a key hub within the default mode network, often receives less attention within addiction research, yet has important implications in the value-based attentional capture during perceptual decision-making, an important aspect in the perpetuation of addictive behaviors. Prior fMRI work has demonstrated

that value-related brain activity in the PCC correlated with the degree by which reaction times of participants were slowed for perceptual choices, suggesting a role of the PCC in automatic value coding and value-driven attentional capture [53]. Research in macaques further supports such role, as PCC neurons were shown to be involved during change detection and policy control during reward-guided behavior while taking into account prior reward experience. [54, 55]. Given prior work within humans and primates for the role of the PCC in value-based decisions, combined with our classification of the PCC as a region distinct to drug cue-reactivity, highlights this region as a potential key constituent in addiction where drugs of abuse may usurp this naturally-rewarding system to shift value towards drug-related cues over natural cues perpetuating the cycle of addiction.

Distributed networks of cue-reactivity. Pharmacological addictions are often conceptualized as having effects on numerous brain circuits and networks, rather than a specific lesion or activation in circumscribed brain regions [56]. The dynamic interactions within and between these various brain networks correspond to alterations in cognitive processes including reward processing, emotion regulation, and attention. As such, we examined the functional profiles, both task-free and task-based, of cue-reactivity regions to elucidate additional regions concurrently engaged, and clustered these functional profiles into cliques, or sub-networks to delineate the multiple elements comprising cue-reactivity. We demonstrate that different sub-networks within the cue-reactivity collective system have functional specialization, each performing a specific aspect of processing and responding to visual cues that may be preferentially and dynamically engaged during specific visual interpretations, emotion responses, or salience attributes of the task. Through data-driven techniques, we identified six cliques with meta-analytic decoding results suggesting functional characterization of visual, executive function, sensorimotor, salience, emotion, and self-referential processing.

Tripartite network integration (Cliques 2, 4, 6). The tripartite network parcellation consists of three large-scale brain networks [57]. The central executive network (CEN), a frontoparietal system with primary nodes in the dorsolateral prefrontal cortex (dlPFC) and lateral posterior parietal cortex (PPC), has been implicated in processing exogenous, attentionally driven cognitive functions [58, 59]. The default mode network (DMN), centered around nodes in the PCC, medial prefrontal cortex (mPFC), medial temporal lobe (MTL), and angular gyrus, is typically deactivated during stimulus-driven cognitive tasks as implicated in ruminations, mind wandering, and reflections on the past [60, 61]. The salience network (SN), anchored in the dorsal ACC and frontoinsular cortex (FIC), has been associated with the orienting attention to internal or external stimuli [62, 63]. The dynamic connectivity between and within these three large-scale brain networks have important implications in examining the neurobiological models of addiction and psychopathology [64, 65].

Cue-reactivity Cliques 2, 4, and 6 identified in the current study, via data-driven techniques, closely correspond to canonical CEN, SN, and DMN respectively. An important concept in how environmental stimuli are processed in the brain is the idea that the brain features a continuous flow of information originating from both exogenous and endogenous sources, requiring control mechanisms to orient, identify, and act upon the most salient stimuli. A key network involved in influencing this moment-to-moment information processing is the SN, where "toggling" between the internally directed DMN and the externally directed CEN has relevant implications for the cognitive deficits often noted in addictions [64]. In many stages of the addiction cycle (i.e., taking, withdrawal, and urge), the insula has been highlighted as a key region, that through its interactions with other brain regions alters affective states (e.g., irritability), motivation (e.g., cue-reactivity), and attention (e.g., goal directed behavior) [66]. Specifically during withdrawal, increased engagement of the insula during abstinence augments normative

network switching that potentially explains the reduction in negative coupling between the DMN and CEN, where typically increased activation in CEN corresponds to increased deactivation of DMN [58, 64]. One of the most implicated functions of the DMN in drug abuse is internal ruminations/thinking about one's internal state and self [67]. Prior work examining the chronic effects associated with prolonged nicotine exposure demonstrated increased coupling within left frontoparietal networks and an mPFC network, associated with attentional control during cue reactivity [68], as well as demonstrating a relationship between enhanced cue-reactivity and increased connectivity between SN regions (e.g., insula and dACC) [69]. These results suggest that aberrant connectivity within and between attentional networks (i.e., CEN) and self-referential networks (i.e., DMN), potentially mediated by the insula (i.e., SN), may explain observed imbalances in cue-reactivity [70, 71].

Perceptual networks (Cliques 1 and 3). Inherent to the cue-reactivity paradigm is the recruitment of visual and sensorimotor systems to actively process visually presented stimuli and recruit initial motor systems for action control. Relevant to the current study outcomes, these perceptual systems demonstrated increased convergent activation for drug-related and natural-reward stimuli as compared to control stimuli during cue-reactivity, suggesting a dissociation for reward-based stimuli. As evidenced by an extensive body of work, the representation of basic visual features such as local contrast, spatial location, and spatial frequency can be significantly modulated by attention, as well as learned associations of stimuli with reward [26, 72]. Further, coupling visual stimuli with a reward improves stimulus detection [73, 74], reduces reaction time [75, 76], and increases stimulus selection [77, 78] even in the absence of attention [79]. The neural mechanism by which rewards may regulate selective plasticity in the visual representation of reward-predicting stimuli is through dopamine signaling [80].

It is conceivable that based on reward history and attentional biases, individuals addicted to drugs would demonstrate increased activation in perceptual systems during the presentation of drug-related stimuli, as compared to control stimuli, during cue-reactivity paradigms. Sensory and motor processes have historically been neglected in the addiction literature, yet these systems may have important implications for the development and/or maintenance of addiction. As emphasized in a review of the significance of sensory and motor processes in treatment of addiction [81], activation during drug-cue presentation in sensorimotor regions was shown to predict relapse [82] and correlate with craving, dependence severity, and automatic motor responses to cues [83, 84]. Additional research utilizing somatosensory cues may contribute to a better understanding of early sensory processing in addiction.

Emotion processing (Clique 5). The final clique we identified as a component of cue-reactivity was dominated by the amygdala. The amygdala is subdivided into two distinct nuclei that have cooperating functions: the basolateral and basomedial nuclei (BLA) that encodes emotional events as reference to sensory-specific features (i.e., Pavlovian conditioning), and the central nuclei (CeN) that encodes more general affective and motivational significance in preparatory conditioning [85]. The coordination of these two nuclei support the role of the amygdala in both appetitive and aversive motivational systems, where activation of these systems has been shown to be regulated by stimulus intensity (i.e., arousal) [86]. An essential component of addiction is the dysregulation of emotional systems in the brain that mediate stress and arousal. Specifically, the amygdala has been shown to play a prominent role in the negative emotional state that underlies the motivation between drug-seeking and compulsive use that categorizes drug addiction as a chronically relapsing disorder [87]. Given the role of amygdala functioning in negative reinforcement and drug-seeking behaviors, it has been proposed that the amygdala underlies craving that is triggered by cues such as places, people, and objects associated with drug

use [88]. As such, the amygdala is an important region involved in the cyclical nature of drug addiction, and its function in drug craving and drug seeking behaviors may shed light on the neural mechanisms underlying cue-reactivity, a key concept in drug relapse.

Limitations. Several potential limitations warrant attention. First, the present meta-analysis was limited to functional neuroimaging experiments, thus restricting any interpretation of underlying synaptic and molecular mechanisms. Second, all meta-analyses are susceptible to biases across the literature and limited to original study design. As such, only significant brain activation peaks were published; therefore, we are limited to drawing conclusions on our data. Published peaks lack information on the original fMRI data from which they were generated (i.e. thresholds). Third, the ALE meta-analytic algorithm fails to take into consideration the size of the cluster identified from the primary studies, resulting in less precise representations than image-based meta-analytic approaches [89]. Habituation has been shown in the amygdala and the OFC following repeated presentation, and all studies included used repeated visual presentation of stimuli [90]. When summing male/female ratios across drug and natural cue-reactivity articles, a gender-discrepancy between the two sets became apparent, where drug-related articles reported about twice as many male participants as there were female participants, and the natural-reward articles were more closely balanced. This discrepancy potentially reflects reports that men are more likely than women to use almost all types of illicit drugs [91], as well as for most age groups, men have higher rates of use or dependence on alcohol and illicit drugs than do women [92]; however, this gender-discrepancy warrants further investigation that is outside the scope of the current study. Finally, behavioral decoding results are restricted by the studies archived in the BrainMap and Neurosynth databases at the time of analysis.

Conclusions. In sum, the current study employed emergent neuroimaging meta-analytic techniques to enhance insight into the brain regions, neurocircuits, and more precise mental

operations linked with cue-reactivity tasks. Through such techniques, we defined common and distinct networks involved in cue-reactivity, identified six cliques comprising the paradigm, and behaviorally classified each clique to provide a functional interpretation. Results parse, and highlight the multifaceted constructs involved in cue-reactivity neural processing, specifically into the tripartite network model, perceptual processing networks, and finally an emotion centered network.

ACKNOWLEDGEMENTS

Primary funding for this project was provided by NIH R01 DA041353; additional support was provided by NSF 1631325, NIH U01 DA041156, NSF CNS 1532061, NIH K01 DA037819, NIH U54 MD012393. Additional funding was provided by the Deutsche Forschungsgemeinschaft (DFG, EI 816/11-1), NIH R01-MH074457, the Helmholtz Portfolio Theme "Supercomputing and Modeling for the Human Brain" and the European Union's Horizon 2020 Research and Innovation Programme under Grant Agreement No. 720270 (HBP SGA1) 785907 (HBP SGA2).

REFERENCES

1. Goldstein, R.Z. and N.D. Volkow, *Dysfunction of the prefrontal cortex in addiction: neuroimaging findings and clinical implications.* Nat Rev Neurosci, 2011. **12**(11): p. 652-69.
2. Robinson, T.E. and K.C. Berridge, *Review. The incentive sensitization theory of addiction: some current issues.* Philos Trans R Soc Lond B Biol Sci, 2008. **363**(1507): p. 3137-46.
3. Noori, H.R., A. Cosa Linan, and R. Spanagel, *Largely overlapping neuronal substrates of reactivity to drug, gambling, food and sexual cues: A comprehensive meta-analysis.* Eur Neuropsychopharmacol, 2016. **26**(9): p. 1419-30.
4. Vollstadt-Klein, S., et al., *Effects of cue-exposure treatment on neural cue reactivity in alcohol dependence: a randomized trial.* Biol Psychiatry, 2011. **69**(11): p. 1060-6.
5. Smith, J. and M. Colgate, *Customer Value Creation: A Practical Framework.* The Journal of Marketing Theory and Practice, 2007. **15**(1): p. 7-23.
6. Drummond, D.C., *What does cue-reactivity have to offer clinical research?* Addiction, 2000. **95**(8s2): p. 129-144.
7. Goldstein, R.Z., & Volkow, N. D., *Drug addiction and its underlying neurobiological basis: neuroimaging evidence for the involvement of the frontal cortex.* American Journal of Psychiatry, 2002. **159**(10): p. 1642-1652.
8. Moeller, S.J. and M.P. Paulus, *Toward biomarkers of the addicted human brain: Using neuroimaging to predict relapse and sustained abstinence in substance use disorder.* Prog Neuropsychopharmacol Biol Psychiatry, 2017.
9. Chase, H.W., et al., *The neural basis of drug stimulus processing and craving: an activation likelihood estimation meta-analysis.* Biol Psychiatry, 2011. **70**(8): p. 785-93.
10. Yalachkov, Y., J. Kaiser, and M.J. Naumer, *Functional neuroimaging studies in addiction: multisensory drug stimuli and neural cue reactivity.* Neurosci Biobehav Rev, 2012. **36**(2): p. 825-35.
11. Courtney, K.E., et al., *Neural substrates of cue reactivity: association with treatment outcomes and relapse.* Addict Biol, 2016. **21**(1): p. 3-22.
12. Gardner, E.L., *Endocannabinoid signaling system and brain reward: emphasis on dopamine.* Pharmacol Biochem Behav, 2005. **81**(2): p. 263-84.
13. Belin, D., et al., *Parallel and interactive learning processes within the basal ganglia: relevance for the understanding of addiction.* Behav Brain Res, 2009. **199**(1): p. 89-102.
14. Tang, D.W., et al., *Food and drug cues activate similar brain regions: a meta-analysis of functional MRI studies.* Physiol Behav, 2012. **106**(3): p. 317-24.
15. Everitt, B.J. and T.W. Robbins, *Neural systems of reinforcement for drug addiction: from actions to habits to compulsion.* Nat Neurosci, 2005. **8**(11): p. 1481-9.
16. Kalivas, P.W. and C. O'Brien, *Drug addiction as a pathology of staged neuroplasticity.* Neuropsychopharmacology, 2008. **33**(1): p. 166-80.
17. Montague, P.R., Hyman, S. E., & Cohen, J. D., *Computational roles for dopamine in behavioural control.* Nature, 2004. **431**(7010): p. 760.
18. Ungless, M.A., Whistler, J. L., Malenka, R. C., & Bonci, A., *Single cocaine exposure in vivo induces long-term potentiation in dopamine neurons.* Nature, 2001. **411**(6837): p. 583-587.
19. Vanderschuren, L.J., Schmidt, E. D., De Vries, T. J., Van Moorsel, C. A., Tilders, F. J., & Schoffelmeer, A. N., *A single exposure to amphetamine is sufficient to induce long-term*

behavioral, neuroendocrine, and neurochemical sensitization in rats. Journal of Neuroscience, 1999. **19**(21): p. 9579-9586.

20. Belin, D. and B.J. Everitt, *Cocaine seeking habits depend upon dopamine-dependent serial connectivity linking the ventral with the dorsal striatum.* Neuron, 2008. **57**(3): p. 432-41.
21. Jedynak, J.P., et al., *Methamphetamine-induced structural plasticity in the dorsal striatum.* Eur J Neurosci, 2007. **25**(3): p. 847-53.
22. Kolb, B., Gorny, G., Li, Y., Samaha, A. N., & Robinson, T. E., *Amphetamine or cocaine limits the ability of later experience to promote structural plasticity in the neocortex and nucleus accumbens.* Proceedings of the National Academy of Sciences, 2003. **100**(18): p. 10523-10528.
23. Volkow, N.D., et al., *Cocaine cues and dopamine in dorsal striatum: mechanism of craving in cocaine addiction.* J Neurosci, 2006. **26**(24): p. 6583-8.
24. Volkow, N.D., et al., *Dopamine increases in striatum do not elicit craving in cocaine abusers unless they are coupled with cocaine cues.* Neuroimage, 2008. **39**(3): p. 1266-73.
25. Engelmann, J.M., et al., *Neural substrates of smoking cue reactivity: a meta-analysis of fMRI studies.* Neuroimage, 2012. **60**(1): p. 252-62.
26. Hanlon, C.A., et al., *Visual cortex activation to drug cues: a meta-analysis of functional neuroimaging papers in addiction and substance abuse literature.* Drug Alcohol Depend, 2014. **143**: p. 206-12.
27. Kuhn, S. and J. Gallinat, *Common biology of craving across legal and illegal drugs - a quantitative meta-analysis of cue-reactivity brain response.* Eur J Neurosci, 2011. **33**(7): p. 1318-26.
28. Schacht, J.P., R.F. Anton, and H. Myrick, *Functional neuroimaging studies of alcohol cue reactivity: a quantitative meta-analysis and systematic review.* Addict Biol, 2013. **18**(1): p. 121-33.
29. Carter, B.L., & Tiffany, S. T. , *Meta-analysis of cue-reactivity in addiction research.* Addiction, 1999. **94**(3): p. 327-340.
30. Sescousse, G., Caldú, X., Segura, B., & Dreher, J. C., *Processing of primary and secondary rewards: a quantitative meta-analysis and review of human functional neuroimaging studies.* Neuroscience & Biobehavioral Reviews, 2013. **37**(4): p. 681-696.
31. Diekhof, E.K., et al., *The role of the human ventral striatum and the medial orbitofrontal cortex in the representation of reward magnitude - an activation likelihood estimation meta-analysis of neuroimaging studies of passive reward expectancy and outcome processing.* Neuropsychologia, 2012. **50**(7): p. 1252-66.
32. Lancaster, J.L., et al., *Bias between MNI and Talairach coordinates analyzed using the ICBM-152 brain template.* Hum Brain Mapp, 2007. **28**(11): p. 1194-205.
33. Eickhoff, S.B., Laird, A. R., Grefkes, C., Wang, L. E., Zilles, K., & Fox, P. T. , *Coordinate-based ALE meta-analysis of neuroimaging data: a random-effects approach based on empirical estimates of spatial uncertainty.* Human brain mapping, 2009. **30**(9): p. 2907.
34. Eickhoff, S.B., et al., *Activation likelihood estimation meta-analysis revisited.* Neuroimage, 2012. **59**(3): p. 2349-61.
35. Laird, A.R., et al., *ALE meta-analysis: controlling the false discovery rate and performing statistical contrasts.* Hum Brain Mapp, 2005. **25**(1): p. 155-64.
36. Nichols, T., et al., *Valid conjunction inference with the minimum statistic.* Neuroimage, 2005. **25**(3): p. 653-60.
37. Nooner, K.B., et al., *The NKI-Rockland Sample: A Model for Accelerating the Pace of Discovery Science in Psychiatry.* Front Neurosci, 2012. **6**: p. 152.

38. Camilleri, J.A., et al., *Definition and characterization of an extended multiple-demand network.* Neuroimage, 2018. **165**: p. 138-147.
39. Griffanti, L., et al., *ICA-based artefact removal and accelerated fMRI acquisition for improved resting state network imaging.* Neuroimage, 2014. **95**: p. 232-47.
40. Salimi-Khorshidi, G., et al., *Automatic denoising of functional MRI data: combining independent component analysis and hierarchical fusion of classifiers.* Neuroimage, 2014. **90**: p. 449-68.
41. Satterthwaite, T.D., et al., *An improved framework for confound regression and filtering for control of motion artifact in the preprocessing of resting-state functional connectivity data.* Neuroimage, 2013. **64**: p. 240-56.
42. Ashburner, J. and K.J. Friston, *Unified segmentation.* Neuroimage, 2005. **26**(3): p. 839-51.
43. Laird, A.R., et al., *Investigating the functional heterogeneity of the default mode network using coordinate-based meta-analytic modeling.* J Neurosci, 2009. **29**(46): p. 14496-505.
44. Robinson, J.L., et al., *Metaanalytic connectivity modeling: delineating the functional connectivity of the human amygdala.* Hum Brain Mapp, 2010. **31**(2): p. 173-84.
45. Fox, P.T., et al., *Meta-analysis in human neuroimaging: computational modeling of large-scale databases.* Annu Rev Neurosci, 2014. **37**: p. 409-34.
46. Laird, A.R., Eickhoff, S. B., Fox, P. M., Uecker, A. M., Ray, K. L., Saenz, J. J., ... & Turner, J. A., *The BrainMap strategy for standardization, sharing, and meta-analysis of neuroimaging data.* BMC research notes, 2011. **4**(1): p. 349.
47. Eickhoff, S.B., et al., *Behavior, sensitivity, and power of activation likelihood estimation characterized by massive empirical simulation.* Neuroimage, 2016. **137**: p. 70-85.
48. Eickhoff, S.B., et al., *Co-activation patterns distinguish cortical modules, their connectivity and functional differentiation.* Neuroimage, 2011. **57**(3): p. 938-49.
49. Timm, N.H., *Applied multivariate analysis*. 2002: Springer-Verlag New York.
50. Marrelec, G., et al., *Partial correlation for functional brain interactivity investigation in functional MRI.* Neuroimage, 2006. **32**(1): p. 228-37.
51. Fox, P.T., & Lancaster, J. L., *Mapping context and content: the BrainMap model.* Nature Reviews Neuroscience, 2002. **3**(4): p. 319.
52. Yarkoni, T., et al., *Large-scale automated synthesis of human functional neuroimaging data.* Nat Methods, 2011. **8**(8): p. 665-70.
53. Grueschow, M., et al., *Automatic versus Choice-Dependent Value Representations in the Human Brain.* Neuron, 2015. **85**(4): p. 874-85.
54. Hayden, B.Y., et al., *Posterior cingulate cortex mediates outcome-contingent allocation of behavior.* Neuron, 2008. **60**(1): p. 19-25.
55. Pearson, J.M., et al., *Posterior cingulate cortex: adapting behavior to a changing world.* Trends Cogn Sci, 2011. **15**(4): p. 143-51.
56. Koob, G.F. and N.D. Volkow, *Neurocircuitry of addiction.* Neuropsychopharmacology, 2010. **35**(1): p. 217-38.
57. Menon, V., *Large-scale brain networks and psychopathology: a unifying triple network model.* Trends Cogn Sci, 2011. **15**(10): p. 483-506.
58. Fox, M.D., et al., *The human brain is intrinsically organized into dynamic, anticorrelated functional networks.* Proc Natl Acad Sci U S A, 2005. **102**(27): p. 9673-8.
59. Honey, C.J., et al., *Network structure of cerebral cortex shapes functional connectivity on multiple time scales.* Proc Natl Acad Sci U S A, 2007. **104**(24): p. 10240-5.
60. Greicius, M.D., et al., *Functional connectivity in the resting brain: a network analysis of the default mode hypothesis.* Proc Natl Acad Sci U S A, 2003. **100**(1): p. 253-8.

61. Qin, P. and G. Northoff, *How is our self related to midline regions and the default-mode network?* Neuroimage, 2011. **57**(3): p. 1221-33.
62. Seeley, W.W., et al., *Dissociable intrinsic connectivity networks for salience processing and executive control.* J Neurosci, 2007. **27**(9): p. 2349-56.
63. Sridharan, D., D.J. Levitin, and V. Menon, *A critical role for the right fronto-insular cortex in switching between central-executive and default-mode networks.* Proceedings of the National Academy of Sciences, 2008. **105**(34): p. 12569-12574.
64. Sutherland, M.T., et al., *Resting state functional connectivity in addiction: Lessons learned and a road ahead.* Neuroimage, 2012. **62**(4): p. 2281-95.
65. Sha, Z., et al., *Common Dysfunction of Large-Scale Neurocognitive Networks Across Psychiatric Disorders.* Biol Psychiatry, 2019. **85**(5): p. 379-388.
66. Naqvi, N.H. and A. Bechara, *The insula and drug addiction: an interoceptive view of pleasure, urges, and decision-making.* Brain Struct Funct, 2010. **214**(5-6): p. 435-50.
67. Steele, V.R., X. Ding, and T.J. Ross, *Addiction: Informing drug abuse interventions with brain networks*, in *Connectomics*. 2019. p. 101-122.
68. Janes, A.C., et al., *Prefrontal and limbic resting state brain network functional connectivity differs between nicotine-dependent smokers and non-smoking controls.* Drug Alcohol Depend, 2012. **125**(3): p. 252-9.
69. Janes, A.C., et al., *Insula-Dorsal Anterior Cingulate Cortex Coupling is Associated with Enhanced Brain Reactivity to Smoking Cues.* Neuropsychopharmacology, 2015. **40**(7): p. 1561-8.
70. McClernon, F.J., et al., *24-h smoking abstinence potentiates fMRI-BOLD activation to smoking cues in cerebral cortex and dorsal striatum.* Psychopharmacology (Berl), 2009. **204**(1): p. 25-35.
71. Fedota, J.R. and E.A. Stein, *Resting-state functional connectivity and nicotine addiction: prospects for biomarker development.* Ann N Y Acad Sci, 2015. **1349**: p. 64-82.
72. Serences, J.T., *Value-based modulations in human visual cortex.* Neuron, 2008. **60**(6): p. 1169-81.
73. Engelmann, J.B., et al., *Combined effects of attention and motivation on visual task performance: transient and sustained motivational effects.* Front Hum Neurosci, 2009. **3**: p. 4.
74. Engelmann, J.B. and L. Pessoa, *Motivation sharpens exogenous spatial attention.* Emotion, 2007. **7**(3): p. 668-74.
75. Nomoto, K., et al., *Temporally extended dopamine responses to perceptually demanding reward-predictive stimuli.* J Neurosci, 2010. **30**(32): p. 10692-702.
76. O'Doherty, J., et al., *Dissociable roles of ventral and dorsal striatum in instrumental conditioning.* Science, 2004. **304**(5669): p. 452-4.
77. Pessiglione, M., et al., *Subliminal instrumental conditioning demonstrated in the human brain.* Neuron, 2008. **59**(4): p. 561-7.
78. Pessiglione, M., et al., *Dopamine-dependent prediction errors underpin reward-seeking behaviour in humans.* Nature, 2006. **442**(7106): p. 1042-1045.
79. Seitz, A.R., D. Kim, and T. Watanabe, *Rewards Evoke Learning of Unconsciously Processed Visual Stimuli in Adult Humans.* Neuron, 2009. **61**(5): p. 700-707.
80. Arsenault, J.T., et al., *Dopaminergic reward signals selectively decrease fMRI activity in primate visual cortex.* Neuron, 2013. **77**(6): p. 1174-86.
81. Yalachkov, Y., J. Kaiser, and M.J. Naumer, *Sensory and motor aspects of addiction.* Behav Brain Res, 2010. **207**(2): p. 215-22.

82. Kosten, T.R., et al., *Cue-induced brain activity changes and relapse in cocaine-dependent patients.* Neuropsychopharmacology, 2006. **31**(3): p. 644-50.
83. Smolka, M.N., et al., *Severity of nicotine dependence modulates cue-induced brain activity in regions involved in motor preparation and imagery.* Psychopharmacology (Berl), 2006. **184**(3-4): p. 577-88.
84. Yalachkov, Y., J. Kaiser, and M.J. Naumer, *Brain regions related to tool use and action knowledge reflect nicotine dependence.* J Neurosci, 2009. **29**(15): p. 4922-9.
85. Balleine, B.W. and S. Killcross, *Parallel incentive processing: an integrated view of amygdala function.* Trends Neurosci, 2006. **29**(5): p. 272-9.
86. Bonnet, L., et al., *The role of the amygdala in the perception of positive emotions: an "intensity detector".* Front Behav Neurosci, 2015. **9**: p. 178.
87. Koob, G.F., *Brain stress systems in the amygdala and addiction.* Brain Res, 2009. **1293**: p. 61-75.
88. Weiss, F., *Neurobiology of craving, conditioned reward and relapse.* Curr Opin Pharmacol, 2005. **5**(1): p. 9-19.
89. Salimi-Khorshidi, G., et al., *Meta-analysis of neuroimaging data: a comparison of image-based and coordinate-based pooling of studies.* Neuroimage, 2009. **45**(3): p. 810-23.
90. Wright, C.I., Fischer, H., Whalen, P. J., McInerney, S. C., Shin, L. M., & Rauch, S. L., *Differential prefrontal cortex and amygdala habituation to repeatedly presented emotional stimuli.* Neuroreport, 2001. **12**(2): p. 379-383.
91. NIDA. *Substance Use in Women*. 2020 [cited 2020 February 24]; Available from: https://www.drugabuse.gov/publications/research-reports/substance-use-in-women.
92. Anthony, J.C., L.A. Warner, and R.C. Kessler, *Comparative Epidemiology of Dependence on Tobacco, Alcohol, Controlled Substances, and Inhalants: Basic Findings From the National Comorbidity Survey.* Experimental and Clinical Psychopharmacology, 1994. **2**(3): p. 244-268.

TABLES

Table 1. Meta-analytic cluster coordinates for each contrast examining the pooled, common, and distinct activity increases associated with the cue-reactivity paradigm.

Cluster	Region	Volume	BA	Side	X	Y	Z
A. Pooled cue-reactivity							
1	amygdala	34112		L	-22	-2	-20
2	*caudate*			*R*	*8*	*12*	*-4*
3	*amygdala*			*R*	*20*	*-4*	*-16*
4	*caudate*			*L*	*-8*	*10*	*-4*
5	*thalamus*			*B*	*0*	*-8*	*4*
6	*insula (A)*			*R*	*36*	*20*	*-12*
7	*putamen*			*R*	*24*	*6*	*0*
8	anterior cingulate (Fp2)	11807	32	L	-4	46	0
9	*anterior cingulate*			*L*	*-2*	*24*	*30*
10	inferior temporal gyrus	9516	37	R	50	-68	-4
11	*inferior occipital gyrus*			*R*	*36*	*-86*	*-8*
12	inferior occipital gyrus	8489	37	L	-48	-70	-6
13	medial orbital gyrus	7251	47	L	-26	34	-16
14	*insula (P)*			*L*	*-40*	*-2*	*4*
15	*insula (A)*			*L*	*-28*	*14*	*-14*
16	inferior parietal lobule	5031	7	R	30	-50	54
17	*middle occipital gyrus*			*R*	*30*	*-70*	*36*
18	inferior frontal gyrus	2681	9	R	48	8	28
19	inferior parietal lobule	2293	7	L	-30	-54	56
20	supramarginal gyrus	2271	40	L	-58	-28	34
21	*inferior parietal lobule (PFt)*			*L*	*-44*	*-36*	*46*
22	inferior temporal gyrus	2067		L	-44	-48	-18
23	posterior cingulate	1695	31	L	-4	-52	26
B. Common cue-reactivity							
1	caudate (head)	2544		R	14	4	-10
2	amygdala	1344		L	-22	-2	-20
3	caudate (head)	1016		L	-8	10	-2
4	thalamus	760		B	0	-12	6
5	inferior temporal gyrus (fusiform gyrus)	656	37	L	-44	-68	-8
6	dACC	408	32	L	-2	46	0
7	ventral ACC	24	24	B	0	34	10
8	dACC	8	32	R	4	40	14
C. Drug distinct convergence							
1	PCC	2767	30	L	-8	-44	26
2	putamen	1116		R	24	10	4
3	fusiform gyrus	661	18	R	30	-96	-8
4	ACC	337		L	-8	50	-6
D. Natural distinct convergence							
1	caudate head	14297		R	2	6	-2
2	middle occipital gyrus	9543	19	R	52	-72	10
3	middle occipital gyrus	6645	37	L	-50	-72	-4
4	superior parietal lobule	5215	7	R	36	-50	52
5	middle frontal gyrus	4407	11	L	-24	32	-20
6	superior parietal lobule	2851	7	L	-26	-68	52
7	subcallosal gyrus	2536	47	R	24	20	-16
8	ACC	2265	32	L	0	40	6
9	postcentral gyrus	1599	2	L	-50	-28	40
10	inferior frontal gyrus	1305	6	R	52	6	28
11	inferior frontal gyrus	485	45	R	40	30	0

Note. Lettering corresponds to contrasts in Figure 1: A, B, C, and D respectively. Cluster coordinates for A, C, and D are based on voxel peak maximum, where coordinates for B are based on center of mass. Italicized regions in section A represent local maxima within each cluster. All cluster coordinates (X, Y, Z) are reported in MNI space. Volume is mm^3.

FIGURES

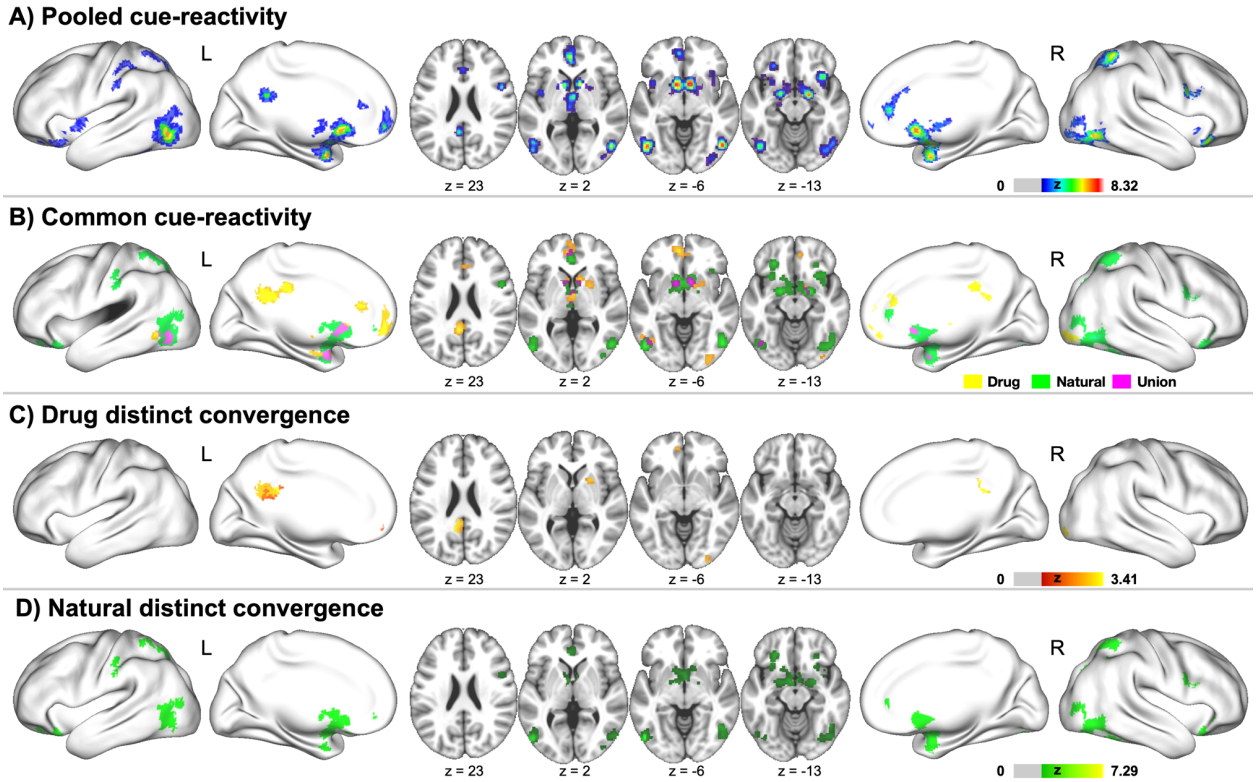

Figure 1. Brain regions showing pooled, common, and distinct activity increase in cue-reactivity paradigms. A) Pooled cue-reactivity (i.e., drug and natural cues collapsed > neutral) was observed in L amygdala, L ACC, L and R ITG, L IOG, L MOG, L and R IPL, R IFG, L SMG, and L PCC. B) Conjunction analysis identified regions associated with drug cues (yellow-gold), natural cues (light blue), and common areas of overlap (pink), including L and R caudate, L amygdala, bilateral thalamus, L ITG, L and R dACC, and bilateral ventral ACC. C) Drug distinct convergence (i.e., drug > natural) was observed in L PCC, R putamen, R ITG, and L ACC. D), while natural distinct convergence (i.e., natural > drug) was observed in R caudate, L and R MOG, L and R superior parietal lobule, L and R IFG, R subcallosal gyrus, L ACC, and L postcentral gyrus. ($p_{\text{cluster-corrected}}<0.05$, $p_{\text{voxel}}<0.001$). IOG = inferior occipital gyrus, IPL = inferior parietal lobule, IFG = inferior frontal gyrus, SMG = supramarginal gyrus.

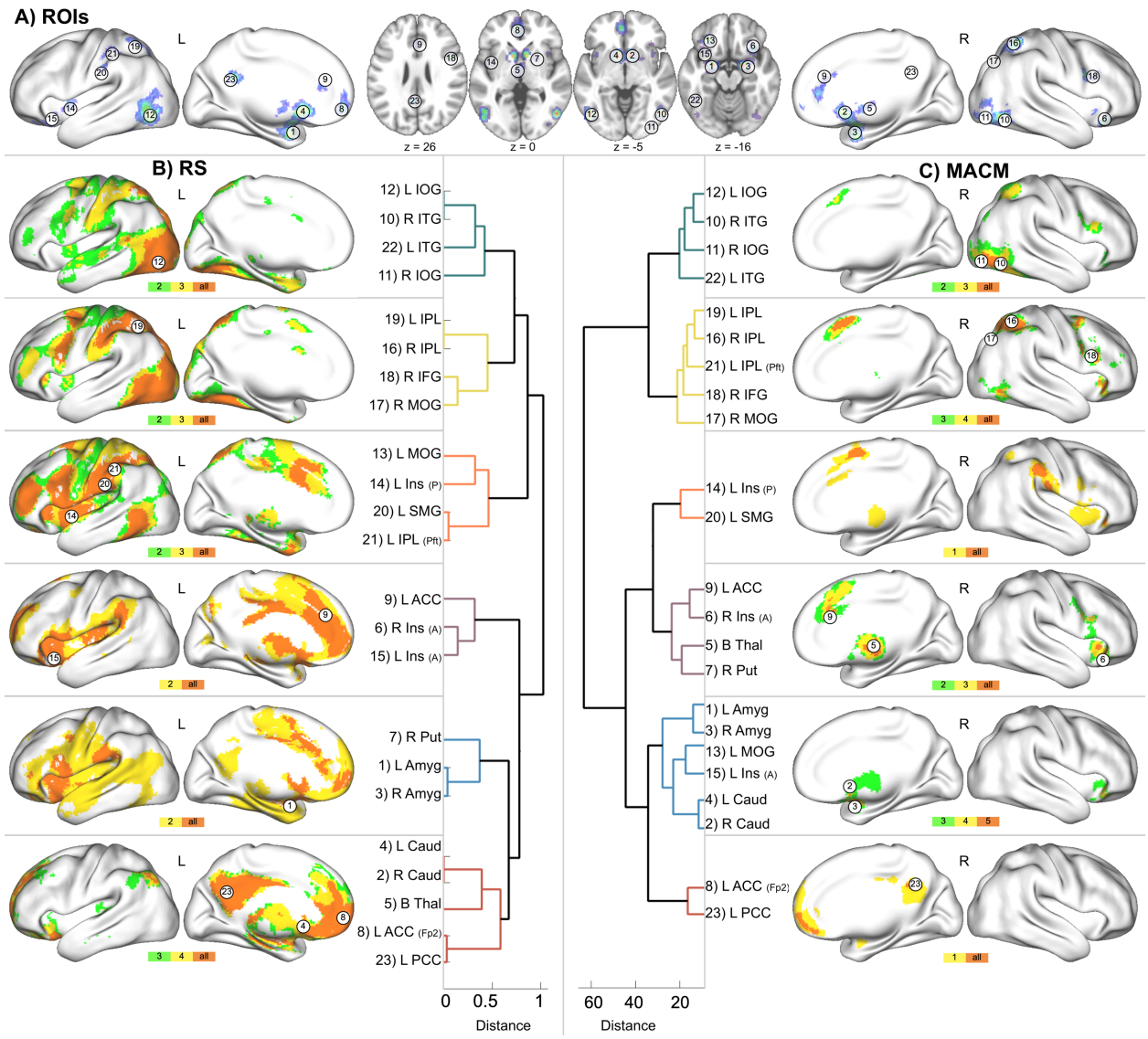

Figure 2. The degree of overlap between regions of interest within a clique for task-free (rsFC) and task-based (MACM) maps. A) Visual representation of the 23 regions of interest associated with cue-reactivity. B-C) Hierarchical clustering on each seed-based functional connectivity pattern defined cliques of regions organized by functional similarity (RS- left, MACM-right). Both rsFC and MACM were defined by six cliques. The horizontal axes represent the dissimilarity between clusters, distance for section B is Ward's linkage distance of the partial correlation coefficients, and distance for section C is Ward's linkage distance of the Euclidean distances between MACMs. Brain images visually represent the degree of overlap for RS (B) and MACM (C) maps within each clique; orange demonstrating the highest degree of overlap (all regions), yellow demonstrating the second degree of overlap, and green demonstrating the lowest degree of overlap.

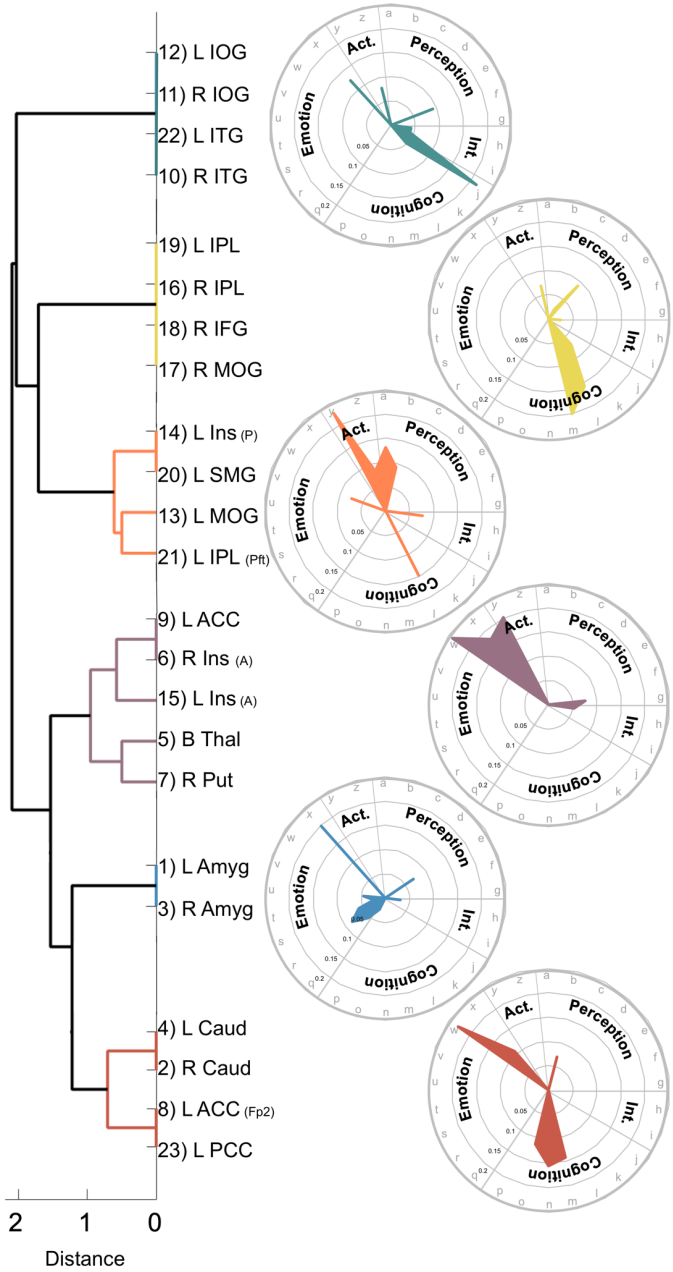

<u>Figure 3.</u> Consensus clustering solution between resting-state and MACM cliques with associated functional decoding behavioral domains and terms. Distance on the x-axis represents Ward's linkage distance of the Dice Similarity Coefficients for clique assignment. As demonstrated by the polar-plots, Clique 1 (green) consisted primarily of behavioral domain categories cognition and interoception. Clique 2 (yellow) consisted primarily of behavioral domain category cognition. Clique 3 (orange) was consistently associated with domains perception and action. Clique 4 (purple) and Clique 5 (blue) were both linked with behavioral domain emotion. Clique 6 (red) was primarily linked with behavioral domain cognition. The letters organized within each clique polar-plot correspond to BrainMap sub-domains (Table S3).

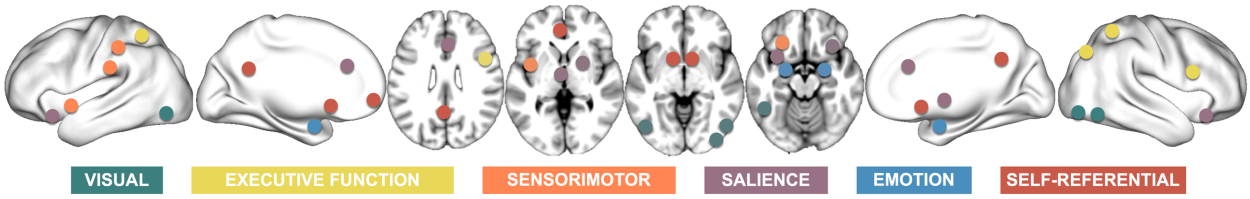

Figure 4. Summary illustration of six cue-reactivity cliques. The cue-reactivity paradigm was delineated into six distinct cliques representing an array of behaviors. Clique 1 (green) included the L and R IOG, and L and R ITG, and was associated with metadata linked to visual processing. Clique 2 (yellow) included the L and R IPL, R IFG, and R MOG, and was associated with metadata linked to executive functions and the central executive network. Clique 3 (orange) included the L insula, L SMG, L MOG, and L IPL, and was shown to be linked with metadata regarding sensorimotor processes. Clique 4 (purple) included the L ACC, L and R insula, B thalamus, and R putamen, regions corresponding to the salience network. Clique 5 (blue) included the L and R amygdala and was associated with metadata related to emotion processing. Finally, Clique 6 (red) included the L and R caudate, L ACC, and L PCC, regions corresponding with the default mode network, and associated with metadata linked to self-referential processing.